Journal of Hydrology 565 (2018) 237–247

Contents lists available at ScienceDirect

Journal of Hydrology

journal homepage: www.elsevier.com/locate/jhydrol

Research papers

Recent rebound in observational large-pan evaporation driven by heat wave and droughts by the Lower Yellow River

Zhigang Sun[a,b,*], Zhu Ouyang[a,b], Junfang Zhao[c], Shiji Li[a,b], Xubo Zhang[a], Wei Ren[d]

[a] Key Laboratory of Ecosystem Network Observation and Modeling, Institute of Geographic Sciences and Natural Resources Research, Chinese Academy of Sciences, Beijing 100101, China
[b] College of Resources and Environment, University of Chinese Academy of Sciences, Beijing 100190, China
[c] State Key Laboratory of Severe Weather, Chinese Academy of Meteorological Sciences, Beijing 100081, China
[d] Department of Plant and Soil Sciences, College of Agriculture, Food and Environment, University of Kentucky, KY 40546-0091, USA

ARTICLE INFO

This manuscript was handled by Marco Borga, Editor-in-Chief, with the assistance of Yuting Yang, Associate Editor

Keywords:
Large pan evaporation
Climatic variables
Extreme Climatic events
Heat wave
Drought

ABSTRACT

Pan evaporation, as a straightforward proxy of potential evapotranspiration, has consistently decreased during the last several decades in many regions across the globe mainly because of global dimming and/or decreases in wind speed. Based on a robust measurement dataset of 30-year large-pan evaporation, however, we found that recent increasing extreme climate events have reversed the decreasing trend in pan evaporation by the Lower Yellow River, with a significant increase of up to 25.2 mm/yr during 2008–2014. Further analyses show that the decrease in large-pan evaporation during 1985–2008 (−5.1 mm/yr) was mainly caused by the decreased vapor pressure deficit (VPD) and sunshine hours. While the sharp increase in large-pan evaporation after 2008 was mainly caused by more frequent heat wave and drought events in spring and summer, which resulted in concurrent increases in air temperature, VPD, and sunshine hours. Our finding of evaporation rebound due to heat wave and droughts calls for improved strategies of water and crop managements for mitigating the negative effects of increasing extreme climate events.

1. Introduction

Pan evaporation has been measured for a few decades in agricultural, hydrological, and climatic sciences as an estimate of the "evaporative demand" of the atmosphere (Rotstayn et al., 2006). Potential evapotranspiration (PET) is the amount of ET that occurs if a sufficient water source is available, which is essential for water resources managements such as agricultural irrigation and water supply (Brutsaert and Parlange, 1998; Ohmura and Wild, 2002; Peterson et al., 1995; Roderick and Farquhar, 2002). Both pan evaporation and PET could quantify the "evaporative demand" of the atmosphere although they differ in acquisition methods (measure vs. calculation) and surfaces (water surface within a pan vs. land surfaces). Thus pan evaporation is commonly used as a proxy of PET. The long-term measurements of pan evaporation are helpful to understand the changes in the atmospheric water demand and to improve water resources managements under changing environments.

Trends in pan evaporation globally reported after 2011 were summarized in Table 1, since global trends in pan evaporation reported before 2011 have been summarized by McVicar et al. (2012). During the last several decades, a decreasing trend in pan evaporation was widely reported in many regions across the globe, for example, USA and Former Soviet Union (Golubev et al., 2001), Canada (Burn and Hesch, 2007), Australia (Roderick and Farquhar, 2004; Roderick et al., 2007), China (Liu et al., 2010; Liu et al., 2011b; Xie et al., 2015; Yang and Yang, 2012; Zhang et al., 2007), India (Jhajharia et al., 2009), and Thailand (Limjirakan and Limsakul, 2012), although some sites showed an increasing trend in pan evaporation (Liu et al., 2010; Liu et al., 2011a; You et al., 2013). Pan evaporation was also reported to persistently decrease in both energy- and water-limited regions, which is reversely consistent with the increasing trend in global averaged air temperature (McVicar et al., 2012). These decreasing trends in pan evaporation across above-mentioned regions were mainly attributed to global dimming (or reduction in solar irradiance) and/or decreases in wind speed (McVicar et al., 2012; Roderick et al., 2007; Wang and Yang, 2014; Wild, 2009). Considered as one of the most interesting trends observed and identified to be associated in some way with climate change, the trend in pan evaporation and its underlying causes and implications for the global hydrologic cycle have attracted broad interests among the scientific community (Brutsaert and Parlange,

* Corresponding author at: Institute of Geographic Sciences and Natural Resources Research, CAS, 11A, Datun Road, Chaoyang District, Beijing 100101, China.
E-mail address: sun.zhigang@igsnrr.ac.cn (Z. Sun).

https://doi.org/10.1016/j.jhydrol.2018.08.014
Received 29 May 2018; Received in revised form 31 July 2018; Accepted 7 August 2018
Available online 14 August 2018

Table 1
Summary of global pan evaporation trends reported after 2011. Studies on pan evaporation trends reported before 2011 had been summarized by McVicar et al. (2012).

Study number	Site or region	Period	Type of pan evaporator	Key findings	Source
1	10 stations in Uruguay	1973–2014	Class A evaporation pan with a diameter of 120.7 cm and a depth of 25 cm	With a high interannual variability, pan evaporation showed insignificant trend ($p > 0.05$) at seasonal and annual scales.	Vicente-Serrano et al., 2018
2	525 stations in Mexico	1961–2010	Class-A pan evaporation	A consistent decline in annual pan evaporation for 1960–1990 ($-3.8\,mm\,yr^{-2}$) and for 1990–2010 ($-2.6\,mm\,yr^{-2}$) was mainly caused by decreases in wind speed and net radiation.	Brena-Naranjo et al., 2017
3	588 stations across China	1960–2005	Φ 20 evaporation pan with a diameter of 20 cm and a depth of 10 cm	Pan evaporation decreased in northwest China and north China, and in the Huaihe and Haihe River basins. Pan evaporation increased in northeastern China. Relative humidity dominated pan evaporation changes.	Zhang et al., 2015
4	26 stations on the Tibetan Plateau	1970–2012	Φ 20 evaporation pan	The decrease in pan evaporation was mostly due to declining wind speed ($-13.7\,mm\,yr^{-2}$) with some contributions from decreasing solar irradiance ($-3.1\,mm\,yr^{-2}$); and the increase of temperature had a large positive effect ($+4.55\,mm\,yr^{-2}$).	Xie et al., 2015
5	9 sites in semi-arid Western Turkey	1975–2006	Class A evaporation pan	Only two sites showed significant linear trends, one in decreasing direction and the other in increasing direction. Area-averaged normalized anomalies of pan evaporation stayed unchanged over the period 1975–2006.	Yesilirmak, 2013
6	Ailaoshan, China	1981–2010	Φ 20 evaporation pan	A positive trend in pan evaporation was observed due to increases in wind speed and sunshine hours, with a much larger increase in the dry season than in the wet season.	You et al., 2013
7	81 stations in arid Northwest China	1958–2010	Φ 20 evaporation pan	Pan evaporation decreased at a rate of $-6.0\,mm\,yr^{-2}$ from 1958 to 1993 mainly due to a decrease in wind speed, and then turned to an upward trend at a rate of $10.7\,mm\,yr^{-2}$ mainly due to increases in wind speed and vapor pressure deficit.	Li et al., 2013
8	28 stations in Thailand	1970–2007	Class A evaporation pan	Pan evaporation declined on average by $7.7\,mm\,yr^{-2}$ mainly due to reduction in wind speed followed by sunshine duration.	Limjirakan and Limsakul, 2012
9	54 stations across China	1961–2001	Φ 20 evaporation pan	Average pan evaporation across China decreased by $3.1\,mm\,yr^{-2}$ mainly caused by a decrease in wind speed in most parts of China and a decrease in global solar radiation in southwest China.	Yang and Yang, 2012
10	9 sites in South Florida	1992–2009	Class A evaporation pan	Based on the decline in humidity and the increasing trend in vapor pressure deficit for the short period of 1992–2009, South Florida appeared to experience increase in evaporation.	Abtew et al., 2011
11	21 tropical stations in Nigeria	1970–2000	Class A evaporation pan	Pan evaporation decreased in all the regions except Sahel region in the first decade; however, pan evaporation increased across Nigeria in the rest decades.	Ogolo, 2011

1998; Kisi, 2015; Lim et al., 2016; Ohmura and Wild, 2002; Peterson et al., 1995; Roderick and Farquhar, 2002; Sherwood and Fu, 2014; Wang et al., 2012).

As shown in Table 1 and McVicar et al. (2012), most measurements of pan evaporation were obtained using the Φ20 evaporation pan with a diameter of 20 cm and a depth of 10 cm in China and the US Class A evaporation pan with a diameter of 120.7 cm and a depth of 25 cm outside of China. Whereas the World Meteorological Organization (WMO) recommends a 20 m^2 evaporation pan as the standard equipment for free water surface evaporation, the raw measurements of both Class A and Φ20 evaporators might not directly record the atmospheric evaporative demand above free water surfaces. The conversion coefficients between the 20 m^2 evaporator and given evaporators are commonly used to calibrate Class A and Φ20 evaporation measurements, but they vary with evaporator types and time (Fu et al., 2004). Therefore, a long-term evaporation record from a 20 m^2 evaporator could provide a straightforward view to understand the atmospheric evaporative demand and its trend.

Recent investigations reported that the decrease trend in pan evaporation measured by the Φ20 evaporator disappeared since 1993 across China (Wang et al., 2017), with a typical case in the arid region of Northwest China where pan evaporation obviously decreased at a rate of −6.0 mm/yr before 1993 and turned to increase at a rate of 10.7 mm/yr after 1993 (Li et al., 2013). The North China Plain (NCP), one of three major grain producing areas in China, has experienced an increase in air temperature at a rate of 0.16 °C per decade during 1985–2014. This warming rate is higher than the global average of 0.13 °C per decade (IPCC, 2013). Recent studies also reveal that climate change in the NCP has led to extreme temperatures, extraordinary rainfall events, and more intense and prolonged droughts (Tao et al., 2016; Yuan et al., 2015). Through the overview of studies on pan evaporation trends until 2018 across the world in Table 1 and McVicar et al. (2012), almost all studies related to pan evaporation trends solely with climatic trends. However, extreme events along with climatic trends have not been well investigated to understand the magnitude and changing trend in pan evaporation.

In this study, therefore, we aim to (1) provide a robust dataset of 30-year pan evaporation observations from a 20 m^2 large tank by the Lower Yellow River, (2) examine changing trends in large-pan evaporation as influenced by climate change and local extreme climate events (heat wave and drought), and (3) explore the underlying mechanisms responsible for recent changes in pan evaporation by the Lower Yellow River in the NCP.

2. Methodology

2.1. Experimental station and database

The observation site (36°56′N, 116°38′E) is located at the Yucheng Comprehensive Experimental Station (YCES) along the north of the Lower Yellow River in the North China Plain (Fig. 1). The YCES is characterized by a semi-humid monsoon climate and a cropping system of winter wheat – summer maize, which can be representative of the NCP. During the study period of 1985–2014, the average annual mean air temperature was approximately 13.4 °C; the average annual precipitation was 576.7 mm/yr; and the average annual large pan evaporation was 939.3 mm/yr at the YCES. The dominant cropping system is winter wheat (prior Oct. – Jun.) followed by summer maize (Jun. – Oct.) around the observation site.

The 15 types of pan evaporator with different depths and areas are scattered in the 30 m × 40 m observation field, within which the ground is covered by short grass between evaporation pans (Fig. 1). Pan evaporation was measured through observing the change in water surface measurements on 8:00 and 20:00 from 1985. The evaporator with an area of 20 m^2 and a depth of 2 m (large-pan) was found to have the closest observational values to the open water surface evaporation (Chin and Zhao, 1995; Fu et al., 2004). The meteorological instruments were installed about 20 m away from the evaporators to record air temperature, air humidity, wind speed and direction, precipitation, sunshine hours, and water evaporation measured by a weighting pan evaporator with a diameter of 20 cm (small-pan, *i.e.*, the Φ20 evaporator). The sensors of air temperature, air humidity, and sunshine hours were installed at the 2 m height. The sensors of wind speed and direction were installed at the 10 m height. The weighting pan evaporator was installed on the ground, which can work during the frozen season. Since both the meteorological observation field and the pan evaporation field are surrounded by croplands with much large areas, the effect of pan evaporation on the meteorological observations could be almost ignored.

Monthly large-pan evaporation data from 1985 to 2014 were collected for yearly and seasonal trend analyses. Considering climatic factors are closely related to pan evaporation, meteorological data, including air temperature (daily mean (Tmean), maximum (Tmax), and minimum (Tmin)), humidity, wind speed, precipitation, sunshine hours, and small-pan evaporation, were collected for attribution analyses. The vapor pressure deficit (VPD) was calculated using air temperature and humidity. The water within the large pan is pumped out and the large pan does not work from later November to later March. Large-pan evaporation data gaps during frozen winter were filled using the Φ20 evaporation records with a calibration coefficient of 0.6. This coefficient was obtained through relating observations between the large pan and the Φ20 evaporation pan during unfrozen seasons.

2.2. Analysis methods

A linear regression method was used to obtain the yearly and seasonal trends and *p* values of large-pan evaporation and related climatic factors. The partial least squares (PLS) regression was used to investigate the attribution of the change in the trend of large-pan evaporation. Climatic factors (temperature, VPD, sunshine hours) closely related to pan evaporation sometimes have good correlations between them. However, the PLS method works even when attributed variables are of multicollinearity (Eriksson et al., 2006; Yu et al., 2012). The variable importance in the projection (VIP) and the Pearson correlation coefficient (*R*) obtained from the PLS analysis were used to measure the strength of the relationships between large-pan evaporation and considered climatic factors, where the climatic factors with VIP scores above 0.8 were identified as important ones for the relationship model. In this study, the MS EXCEL V2010 (Microsoft, USA) and SIMCA-P + V11 (Umetrics AB, Sweden) were used for linear regression and PLS analyses.

The STARDEX tool was used to calculate about 40 climatic indices of temperature and rainfall (see https://crudata.uea.ac.uk/projects/stardex/ for details about the STARDEX, accessed on Mar. 1, 2017). Some typical extreme climate indices were used to investigate local prevailing extreme climate events of heat wave and drought, including mean Tmax (txav), Tmax 90th percentile (txq90), mean dry-day persistence (ppdd) defined as the ratio of the total number of consecutive dry days to the total number of dry days for a given period, and mean of dry spell lengths (pdsav).

3. Results

3.1. Changing trends in large-pan evaporation during 1985–2014

The 30-year time-series of yearly and seasonal large-pan evaporation derived from the monthly large-pan evaporation dataset from 1985 to 2014 were used to obtain the values of trend and *p* through a linear regression method. Two distinct trends in yearly large-pan evaporation were found during 1985–2008 and 2008–2014, respectively (Fig. 2).

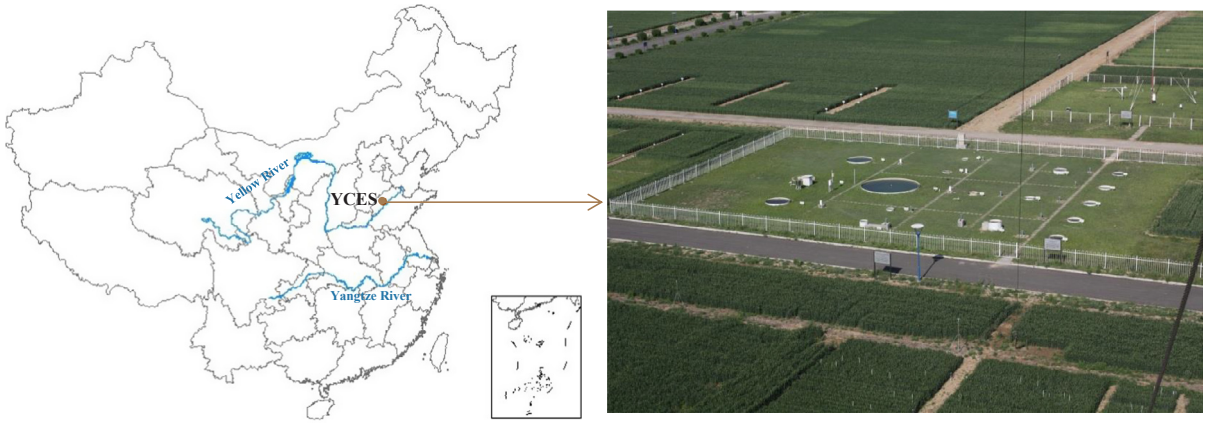

Fig. 1. Observation site and instruments for pan evaporation and meteorological observations.

3.1.1. Annual pattern

Yearly large-pan evaporation had a significantly decreasing trend during 1985–2008, with a trend of −0.014 mm/day/yr (*i.e.*, −5.1 mm/yr) and a *p*-value of 0.0014. Whereas, yearly large-pan evaporation turned to a sharply increasing trend during 2008–2014, with a trend of 0.069 mm/day/yr (*i.e.*, 25.2 mm/yr) and a *p*-value of 0.0053. The magnitude of the increasing trend in yearly large-pan evaporation during 2008–2014 is nearly five times that of the decreasing trend during 1985–2008.

3.1.2. Seasonal pattern

Spring (Mar., Apr., and May), summer (Jun., Jul., and Aug.), and autumn (Sep., Oct., Nov.) large-pan evaporation had the same pattern to yearly large-pan evaporation (Fig. 3). The large-pan evaporation in spring, summer, and autumn during 1985–2008 decreased in trends of −0.012 mm/day/yr (*i.e.*, −1.1 mm/yr, $p = 0.072$), −0.029 mm/day/yr (*i.e.*, −2.7 mm/yr, $p = 0.0067$), and −0.015 mm/day/yr (*i.e.*, −1.4 mm/yr, $p = 0.028$), respectively (Table S1). Whereas, the large-pan evaporation in spring, summer, and autumn during 2008–2014 increased in relatively larger trends of 0.11 mm/day/yr (*i.e.*, 10.1 mm/yr, $p = 0.015$), 0.086 mm/day/yr (*i.e.*, 7.9 mm/yr, $p = 0.18$), and 0.056 mm/day/yr (*i.e.*, 5.1 mm/yr, $p = 0.041$). The large-pan evaporation in winter (Dec., Jan., and Feb.) had no obvious changing trend during 1985–2008, with a trend value of 0.0019 mm/day/year (*i.e.*, 0.17 mm/yr, $p = 0.51$), but had relatively obvious increasing trend during 2008–2014, with a trend value of 0.021 mm/day/year (*i.e.*, 1.9 mm/yr, $p = 0.47$).

3.1.3. Monthly pattern

During 1985–2008, as shown in Fig. 4, large-pan evaporation records of 9 months except Feb., Mar., and Nov. show decreasing trends at the range from −0.0002 mm/day/yr in Dec. (*i.e.*, −0.02 mm/yr) to −0.033 mm/day/yr in Jul. (*i.e.*, −1.02 mm/yr) and the trends in Apr., Jul., Aug., and Sep. (−0.025 mm/day/yr ~ −0.033 mm/day/yr) are statistically significant ($p < 0.05$). During 2008–2014, large-pan evaporation records of 11 months except Feb. show increasing trends at the range from 0.022 mm/day/yr in Jun. (*i.e.*, 0.66 mm/yr) to 0.13 mm/day/yr in Mar. and Aug. (*i.e.*, 4.03 mm/yr), but all trends are statistically non-significant ($p > 0.05$). At the monthly scale, the magnitude of the increasing trend in large-pan evaporation during 2008–2014 is much greater than that of the decreasing trend during 1985–2008.

In summary, spring, summer, autumn, and winter large-pan evaporation during 1985–2008 contributes to the yearly decreasing trend in proportions of 22%, 53%, 28%, and −3%, respectively; whereas spring, summer, autumn, and winter large-pan evaporation during 2008–2014 contributes to the yearly increasing trend in proportions of 40%, 32%, 20%, and 8%, respectively.

3.2. Relative contributions of climatic factors to changes in large-pan evaporation during 1985–2014

Following the Penman equation for calculating evaporation from open water surfaces, large-pan evaporation positively correlates to air temperature, VPD, solar radiation, and wind speed. In this study, the relationships between large-pan evaporation and related factors (air temperature, VPD, sunshine hours, and wind speed) were investigated to understand the attributions of the changing trends in large-pan

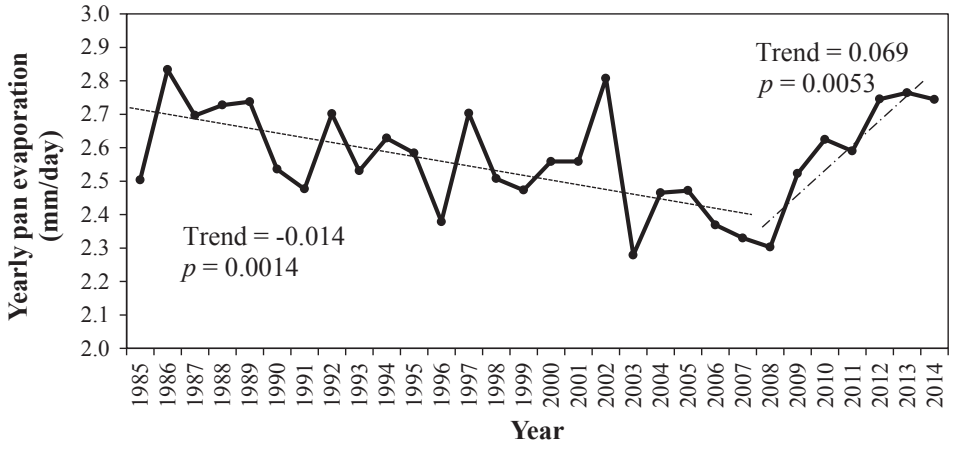

Fig. 2. Yearly large-pan evaporation and its trend (mm/day/yr) at the YCES during 1985–2008 and 2008–2014.

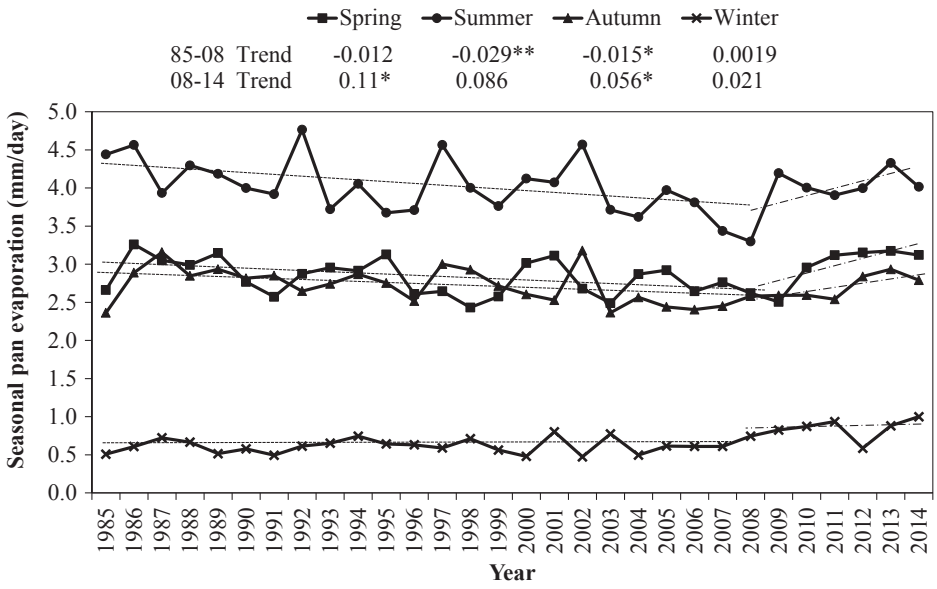

Fig. 3. Large-pan evaporation of 4 seasons and their trends (mm/day/yr) at the YCES during 1985–2008 and 2008–2014 (* indicates $p < 0.05$ and ** indicates $p < 0.01$).

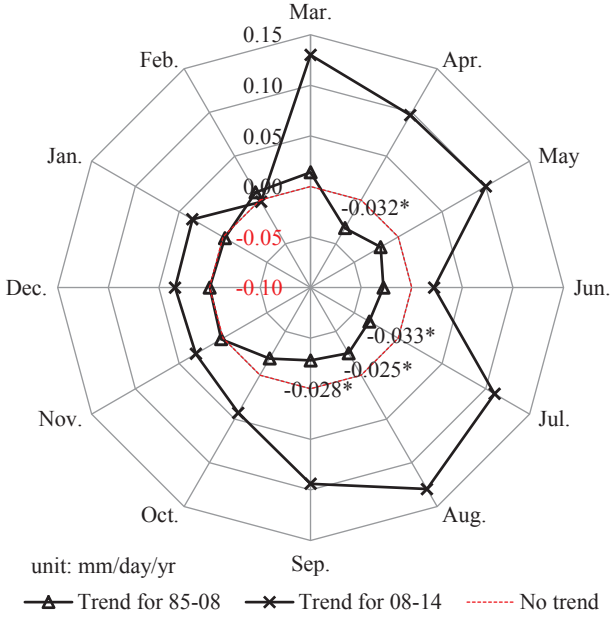

Fig. 4. Changing trends (mm/day/yr) in monthly large-pan evaporation at the YCES during 1985–2008 and 2008–2014. Data points inside the red dashed round indicate a decreasing trend, data points outside the red dashed round indicate an increasing trend, and data points with significant trends are labelled using asterisked values (* indicates $p < 0.05$ and ** indicates $p < 0.01$). (For interpretation of the references to colour in this figure legend, the reader is referred to the web version of this article.)

evaporation during the past 30 years (Fig. 5). The PLS method was used to analyze large-pan evaporation vs. air temperature, VPD, sunshine hours, and wind speed at the yearly, seasonal, and monthly scales, respectively.

On the yearly scale, as shown in Fig. 6 and Tables S2–S5, the decreasing VPD (VIP = 1.13, $R = 0.51^{*}$) and sunshine hours (VIP = 1.50, $R = 0.68^{**}$) significantly contributed to decreasing large-pan evaporation during 1982–2008. However, only air temperature (VIP = 0.45, $R = 0.18$) had a positive and non-significant contribution to the increasing trend in yearly large-pan evaporation during 2008–2014.

On the seasonal scale, as shown in Fig. 7 and Tables S2-S5, air temperature in summer and winter (VIP ≥ 1, $R \geq 0.59^{**}$), VPD in four seasons (VIP ≥ 1.19, $R \geq 0.64^{**}$), and sunshine hours in spring, summer, and autumn (VIP ≥ 1.07, $R \geq 0.64^{**}$) had significant contributions to the decreasing trends in seasonal large-pan evaporation during 1985–2008. Whereas, air temperature (VIP = 1.18, $R = 0.76^{**}$) and sunshine hours (VIP = 1.24, $R = 0.59^{*}$) in summer had significant contributions to the increasing trends in summer large-pan evaporation during 2008–2014.

On the monthly scale, as shown in Fig. 8 and Tables S2–S5, the decreasing trends in monthly large-pan evaporation during 1985–2008 significantly positively correlate to air temperature in Jan., Feb., Mar., May, Jun., and Jul. (VIP ≥ 0.87, $R \geq 0.55^{**}$), VPD in all months (VIP ≥ 1.18, $R \geq 0.46^{*}$), sunshine hours in all months (VIP ≥ 0.90, $R \geq 0.44^{*}$), and wind speed in May, Sep., and Oct. (VIP ≥ 0.81, $R \geq 0.48^{*}$). Whereas, the increasing trends in monthly large-pan evaporation during 2008–2014 were significantly positively correlated to air temperature in Jun. and Aug. (VIP ≥ 1.25, $R \geq 0.86^{*}$), VPD in Jun. (VIP = 1.08, $R = 0.78^{*}$), sunshine hours in May, Jun., and Dec. (VIP ≥ 1.12, $R \geq 0.81^{*}$), and wind speed in May, Sep., and Oct. (VIP ≥ 0.81, $R \geq 0.48^{*}$).

In summary, the decreasing large-pan evaporation during 1985–2008 were mainly caused by the decreasing VPD and sunshine hours in all months and air temperature and wind speed in several months; whereas the sharply increasing large-pan evaporation during 2008–2014 are mainly caused by the increasing air temperature, VPD, and sunshine hours in spring and summer.

3.3. Relations between recent extreme events and rapid rebound in large-pan evaporation after 2008

Recently, heat wave and drought frequently occurred in spring and summer in the NCP (Tao et al., 2016; Yuan et al., 2015), which may cause increases in concurrent air temperature and VPD and then cause increase in large-pan evaporation. Therefore, we further investigated extreme climate events using temperature- and precipitation-related extreme indices during 1985–2014.

3.3.1. Heat wave evidences were explored using temperature-related extreme indices

Some numerical characteristics of the mean Tmax (txav) and the Tmax 90th percentile (txq90) during a given period could indicate the

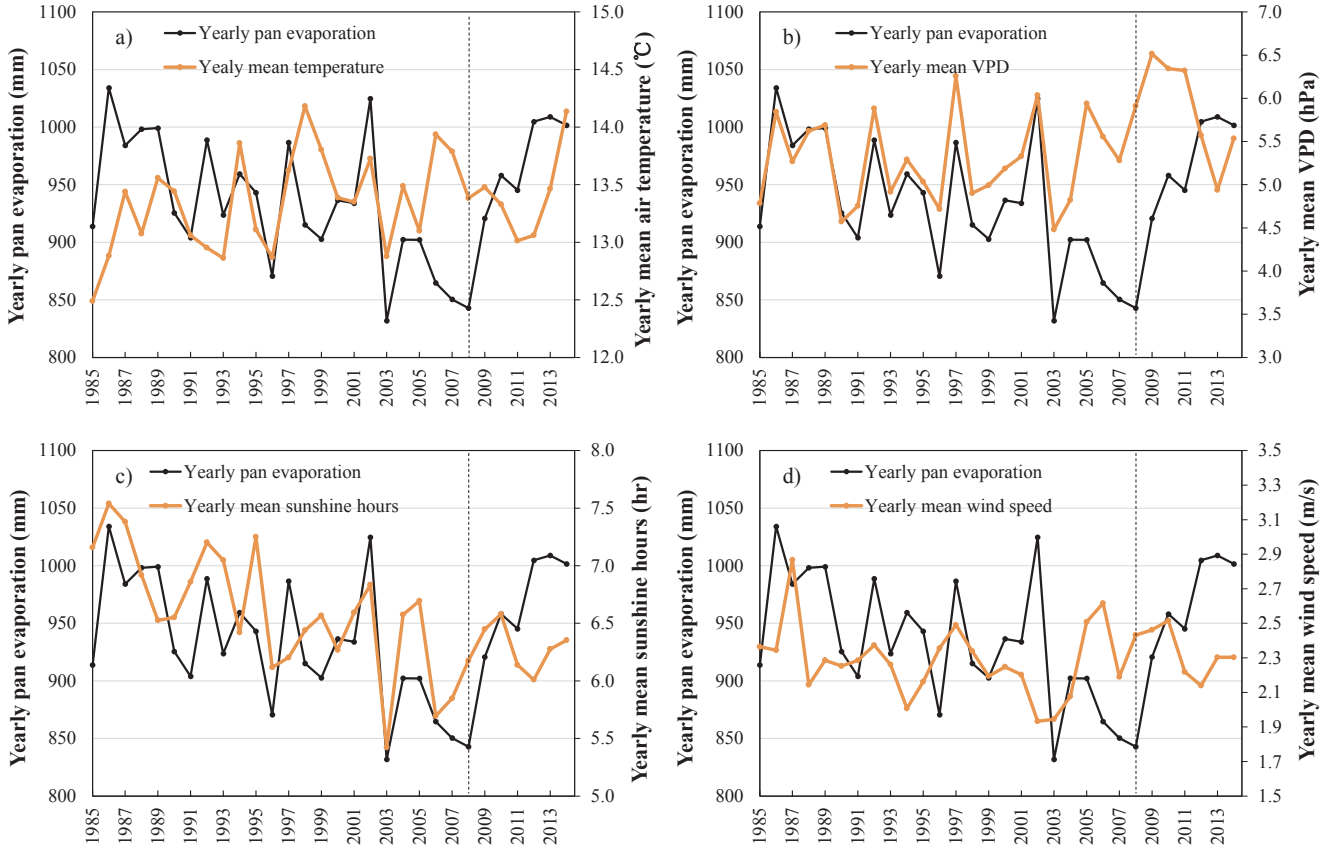

Fig. 5. Yearly large-pan evaporation vs. yearly mean a) temperature, b) VPD, c) sunshine hours, and d) wind speed at the YCES during 1985–2008 and 2008–2014.

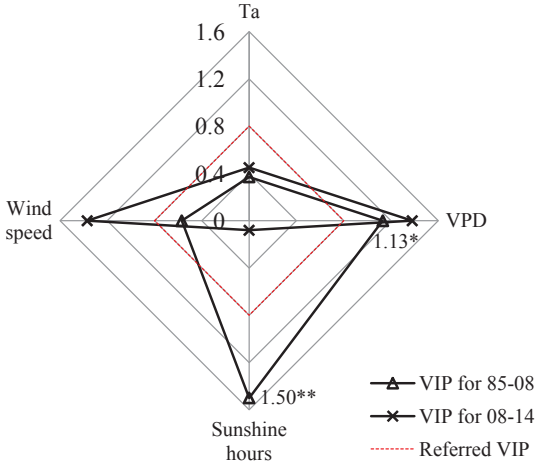

Fig. 6. The scores of variable importance for the projection (VIP) derived from the partial least squares regression (PLS) for yearly large-pan evaporation vs. Ta, VPD, sunshine hours, and wind speed at the YCES during 1985–2008 (85–08) and 2008–2014 (08–14). Data points outside the red dashed round (VIP = 0.8) indicate important climatic factors for the relationship model. Data points passing significance inspection are labelled using asterisked values (* indicates $p < 0.05$ and ** indicates $p < 0.01$). (For interpretation of the references to colour in this figure legend, the reader is referred to the web version of this article.)

duration and intensity of heat wave. Table 2 shows that the txav and txq90 sharply increased in spring and summer during 2008–2014. The trend (Trend = 0.21 °C/yr, $p = 0.65$) in spring txav during 2008–2014 is about 4 times that during 1985–2008. Furthermore, the trend (Trend = 0.16 °C/yr, $p = 0.02$) in summer txav during 2008–2014 is 16 times that during 1985–2008. The trend in txq90 also shows sharp increases in spring (Trend = 0.36 °C/yr, $p = 0.36$) and summer (Trend = 0.15 °C/yr, $p = 0.65$) during 2008–2014. After offsetting the decreasing trends in autumn and winter txq90, the increasing trends in spring and summer txq90 still contribute to a significant increase in yearly txq90 (Trend = 0.21 °C/yr, $p = 0.05$). Remarkable increases in daily maximum temperature and its 90th percentile in spring and summer during 2008–2014 suggest that concurrent heat wave occurred with longer duration or higher intensity.

3.3.2. Drought evidences were explored using precipitation-related extreme indices

Precipitation-related extreme indices of the mean dry-day persistence (ppdd) and the mean of dry spell lengths (pdsav) can be used to quantify the duration and intensity of drought. Table 3 shows that the yearly ppdd and pdsave significantly increased with the trends of 0.01/yr ($p = 0.05$) and 0.46 days/yr ($p = 0.05$) during 2008–2014, respectively. The yearly trends of ppdd and pdsave during 2008–2014 were mainly attributed to their sharp increases in spring and summer although their statistical levels are not significant. The above statistical results indicate that the total number of consecutive dry days and dry spell lengths significantly increased in recent spring and summer. This suggests that both frequency and duration of drought increased in spring and summer during 2008–2014.

3.3.3. The rapid rebound in large-pan evaporation after 2008 was explored against heat wave and drought in spring and summer

The above evidences of increasing heat wave and drought events in spring and summer are closely related to concurrent changes in air temperature, VPD, sunshine hours. Heat wave and drought would increase air temperature and VPD. Heat wave and drought commonly occur in cloudless or less cloud days, which could result in longer sunshine hours. Consequently, the increases in these factors then would

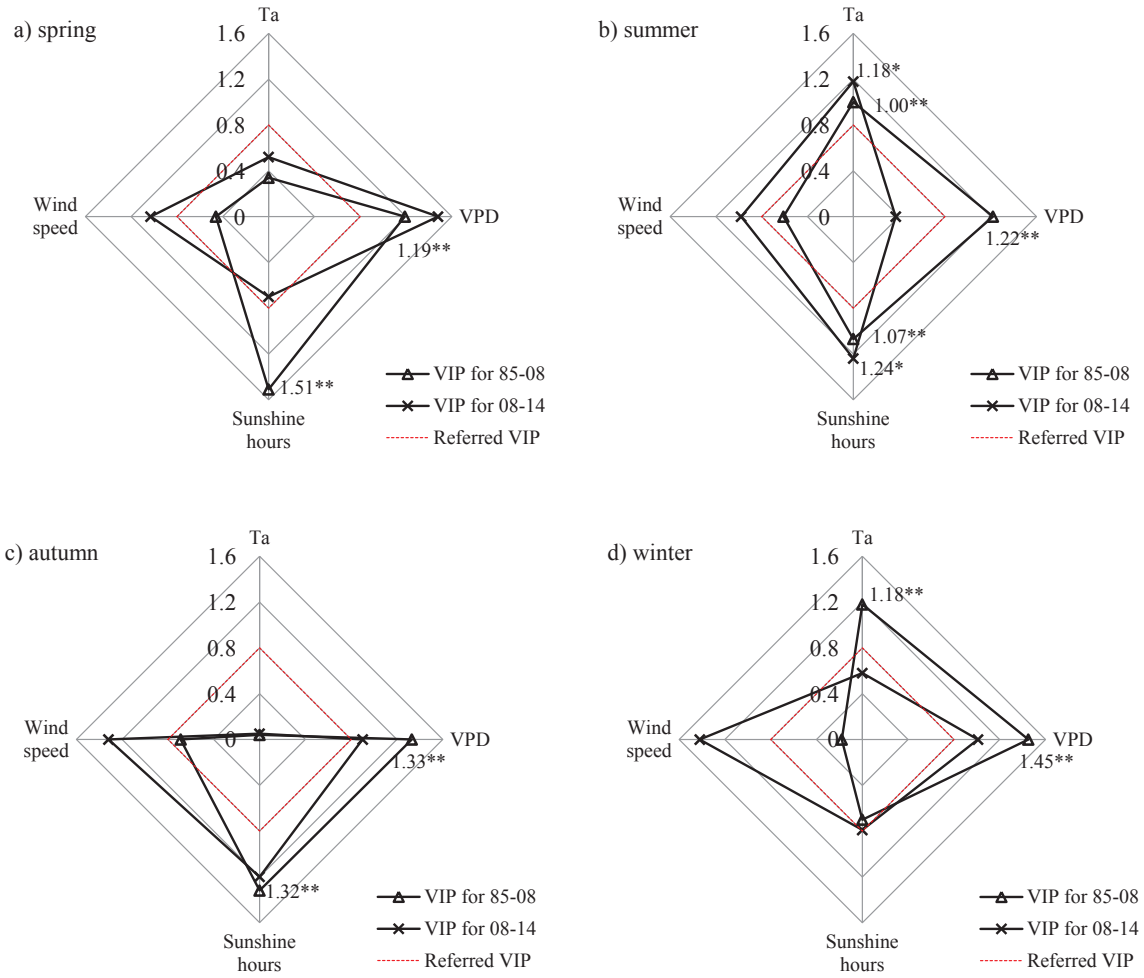

Fig. 7. The scores of variable importance for the projection (VIP) derived from the partial least squares regression (PLS) for seasonal large-pan evaporation vs. Ta, VPD, sunshine hours, and wind speed at the YCES during 1985–2008 (85–08) and 2008–2014 (08–14). Data points outside the red dashed round (VIP = 0.8) indicate important climatic factors for the relationship model. Data points passing significance inspection are labelled using asterisked values (* indicates $p < 0.05$ and ** indicates $p < 0.01$). (For interpretation of the references to colour in this figure legend, the reader is referred to the web version of this article.)

accelerate large-pan evaporation (Figs. 7 and 8). Fig. 9 shows straightforward relations of large-pan evaporation and four extreme climatic indices during 2008–2014. Spring large-pan evaporation significantly correlates to spring droughts, with an R of 0.94^{**} for ppdd and an R of 0.89^{**} for pdsav, whereas summer large-pan evaporation significantly correlates to summer heat waves, with an R of 0.94^{**} for txav and an R of 0.80^{*} for txq90. Subsequently, yearly large-pan evaporation significantly correlates to ppdd, pdsav, and txq90, with R values of ≥ 0.77 ($p < 0.05$). Finally, it could be inferred that recent increasing extreme events of heat wave and drought in spring and summer contributed prevailingly to inversing from the decreasing trend in large-pan evaporation during 1985–2008.

4. Discussion

4.1. Effect of pan evaporator types on evaporation measurement

Pan evaporation measurements vary with evaporation pan types. The 1985–2014 pan evaporation records from the 20 m^2, Φ20, and Class A pans at the YCES station show distinct differences in amplitude on yearly and monthly scales (Fig. 10). In a previous study, the 15 types of evaporation pans were used for pan evaporation observation about 225 km south to the YCES station during 1985–1990, including a widely-used Class A evaporation pan and a 20 m^2 evaporation tank (Fu et al., 2004). The 20 m^2 evaporation tank is suggested as the standard equipment for free water surface evaporation by the World Meteorological Organization (Chin and Zhao, 1995; Fu et al., 2004). Converting measurements of other pan evaporators to free water surface evaporation involves conversion coefficients by reference to the measurements of the 20 m^2 pan evaporator. These conversion coefficients are commonly given as constants although they are affected by installation methods, evaporator structure, manufacturing materials, and meteorological factors such as wind speed and relative humidity (Chin and Zhao, 1995; Fu et al., 2004; Pereira et al., 1995). In this study, therefore, the 30-year measurements of the 20 m^2 pan evaporator provide a straightforward dataset for investigating the vapor flux from the lands to the atmosphere, avoiding the potential errors derived from the use of small pan evaporation measurements and constant conversion coefficients. This dataset can be also used to evaluate model-based pan evaporation analyses.

Pan evaporation records show a similar rebound trend among three evaporator types of the 20 m^2, Φ20, and Class A pans although they have different amplitudes. Compared with the rebound trend of the 20 m^2 pan evaporation during 2008–2014, the Φ20 pan evaporation shows a stronger rebound with a trend of 48.9 mm/yr (*i.e.*, 0.13 mm/day/yr, $p < 0.01$) while the Class A pan evaporation shows a moderate rebound with a trend of 6.2 mm/yr (*i.e.*, 0.017 mm/day/yr, $p < 0.05$). Therefore, it is suggested that pan evaporation measurements from various pan types might present consistent trends but with different evaporation values.

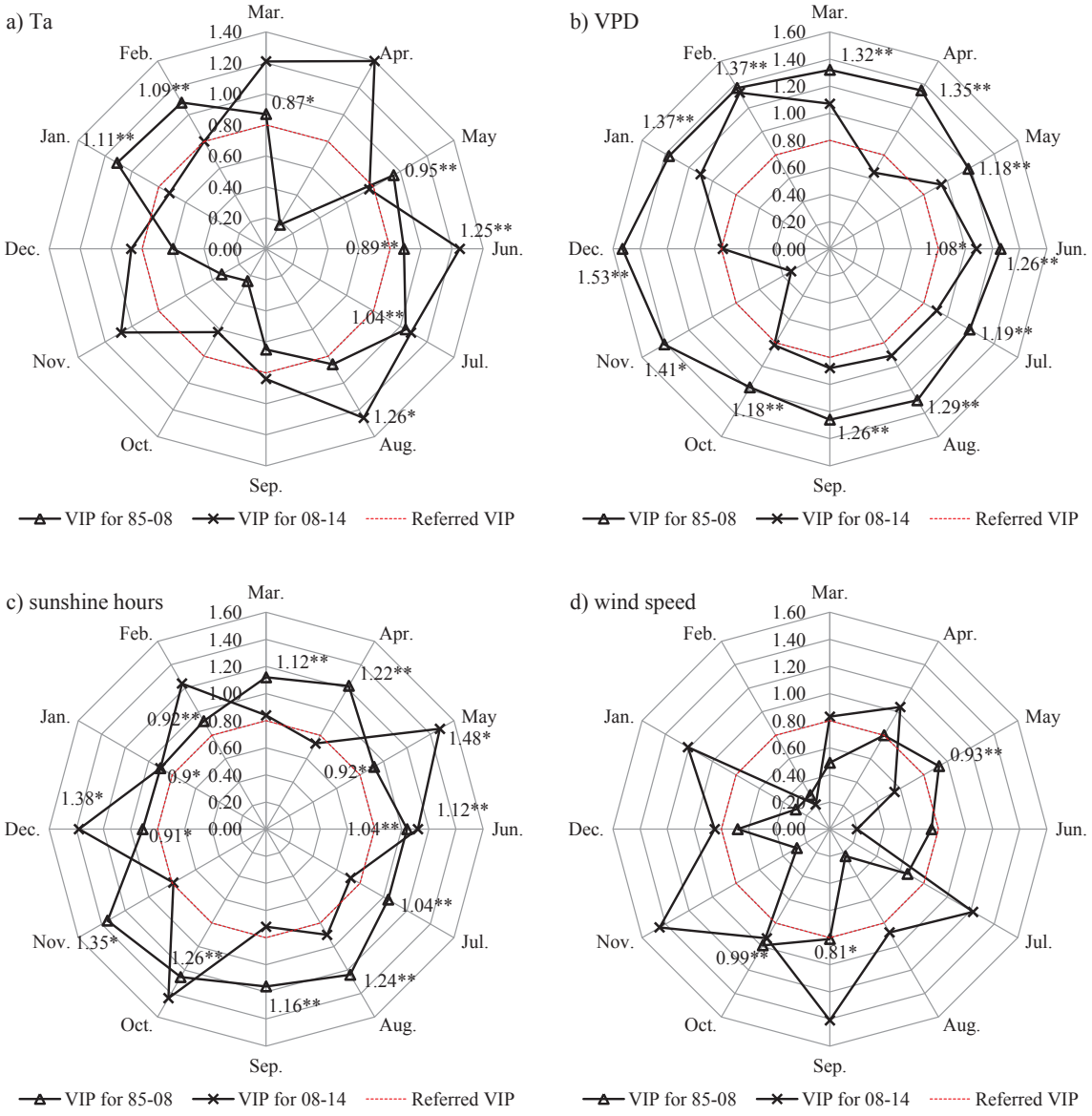

Fig. 8. The scores of variable importance for the projection (VIP) derived from the partial least squares regression (PLS) for monthly large-pan evaporation vs. a) Ta, b) VPD, c) sunshine hours, and d) wind speed at the YCES during 1985–2008 (85–08) and 2008–2014 (08–14). Data points outside the red dashed round (VIP = 0.8) indicate important climatic factors for the relationship model. Data points passing significance inspection are labelled using asterisked values (* indicates $p < 0.05$ and ** indicates $p < 0.01$). (For interpretation of the references to colour in this figure legend, the reader is referred to the web version of this article.)

Table 2
Yearly and seasonal trend and *p*-value of temperature-related indices for heat wave investigation at the YCES during 1985–2008 (85–08) and 2008–2014 (08–14).

Mean Tmax (txav)

	Trend(°C/yr)		*p*-value			Trend(°C/yr)		*p*-value	
	85–08	08–14	85–08	08–14		85–08	08–14	85–08	08–14
Yearly	0.03	0.10	0.07	0.65	Spring	***0.05***	0.21	***0.04***	0.65
					Summer	0.01	***0.16***	0.92	***0.02***
					Autumn	0.03	0.04	0.40	0.88
					Winter	0.02	−0.23	0.41	0.57

Tmax 90th percentile (txq90)

	Trend(°C/yr)		*p*-value			Trend(°C/yr)		*p*-value	
	85–08	08–14	85–08	08–14		85–08	08–14	85–08	08–14
Yearly	0.00	***0.21***	0.82	***0.05***	Spring	−0.003	0.36	0.94	0.36
					Summer	0.03	0.15	0.48	0.65
					Autumn	0.06	−0.16	0.08	0.65
					Winter	0.07	−0.42	0.08	0.35

Note: Boldface italic font for trend and *p* numbers while *p*-value is < 0.05.

Table 3
Yearly and seasonal trend and *p*-value of precipitation-related indices for drought investigation at the YCES during 1985–2008 (85–08) and 2008–2014 (08–14).

Mean dry-day persistence (ppdd)

	Trend		*p*-value			Trend		*p*-value	
	85–08	08–14	85–08	08–14		85–08	08–14	85–08	08–14
Yearly	0.00	***0.01***	0.57	***0.05***	Spring	−0.0008	0.01	0.28	0.10
					Summer	0.0001	0.01	0.90	0.29
					Autumn	−0.0006	0.0016	0.40	0.65
					Winter	0.00	−0.01	0.73	0.44

Mean of dry spell lengths (pdsav)

	Trend(days/yr)		*p*-value			Trend(days/yr)		*p*-value	
	85–08	08–14	85–08	08–14		85–08	08–14	85–08	08–14
Yearly	−0.04	***0.46***	0.47	***0.05***	Spring	−0.08	0.85	0.17	0.10
					Summer	0.02	0.24	0.94	0.29
					Autumn	−0.13	0.58	0.37	0.88
					Winter	−0.11	−2.47	0.96	0.57

Note: Boldface italic font for trend and *p* numbers while *p*-value is less than 0.05.

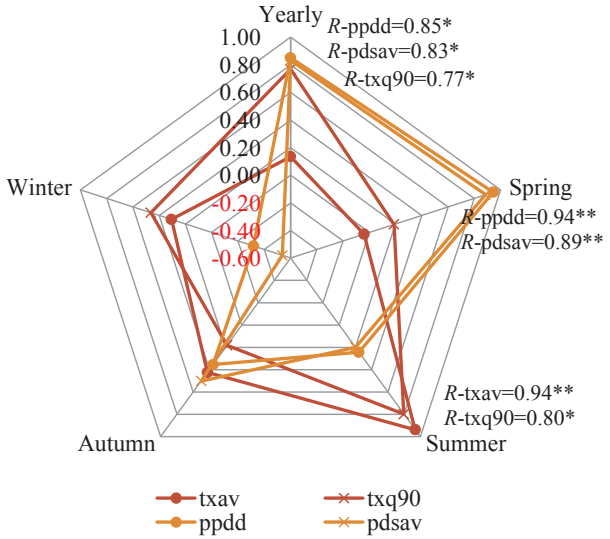

Fig. 9. Correlation coefficient (*R*) from the correlation analyses of large-pan evaporation against four extreme climatic indices on yearly and seasonal scales at the YCES during 2008–2014 (* indicates $p < 0.05$ and ** indicates $p < 0.01$).

4.2. Impact of climatic change and extreme climate events on pan evaporation

The decreasing trends of sunshine hours, VPD, and wind speed before 2008 resulted in the continuous decrease in pan evaporation at the YCES. This attribution is partially supported by previous studies, which found that the decreasing trend in pan evaporation across many regions of the global could be attributed to the decreases in solar radiation and/or wind speed (McVicar et al., 2012; Roderick et al., 2007; Wang and Yang, 2014; Wild, 2009). The decrease in solar radiation was mainly caused by the increase in atmospheric aerosol in the NCP (Wang and Yang, 2014). Farmland expansion and irrigation could cause the increase in air humidity and then the decrease in VPD (Douglas et al., 2006).

Some previous studies have reported an increasing trend in pan evaporation in China; such as You et al. (2013) suggested that southwestern China experienced an increase in pan evaporation during 1981–2010 mainly caused by the increases in wind speed and sunshine hours; Liu et al. (2011a) indicated an increase in pan evaporation in eight climatic regions due to temperature increase during the period of the early 1990s to 2007. In this study, we found that the recent rebound of large-pan evaporation in the NCP was mainly caused by the increasing heat wave and drought events in spring and summer, which has not been reported to date.

4.3. Potential impacts of pan evaporation rebound

The rapid rebound of large-pan evaporation will bring us new issues. The potential water flux from the land to the atmosphere would increase. Pan evaporation could be used to estimate actual ET using empirical coefficients. This indicates that more water might be required for more actual ET to sustain high crop yields. The NCP is one of three major regions of grain production in China, where crop yields mainly depend on precipitation and irrigation. The increasing heat wave and drought is changing the magnitude and frequency of precipitation and potential irrigation demands. With the purpose of adapting to increasing extreme events of heat wave and drought, therefore, the finding of this study suggests that it is urgent to adopt the strategies of water and crop managements to mitigate the negative effects of extreme climate events on crops.

5. Conclusions

Pan evaporation is a straightforward proxy of the potential water flux from the land to the atmosphere. In this study, a robust 30-year dataset of large-pan evaporation was built to investigate changes in pan evaporation at the monthly, seasonal, and yearly time steps in the North China Plain. We found that yearly large-pan evaporation significantly decreased with a trend of −5.1 mm/yr during 1985–2008, to which spring, summer, autumn, and winter large-pan evaporation contributed in proportions of 22%, 53%, 28%, and −3%, respectively. This decreasing trend in large-pan evaporation was mainly caused by the decreasing VPD and sunshine hours. Whereas, large-pan evaporation significantly increased with a trend of up to 25.2 mm/yr during 2008–2014, to which spring, summer, autumn, and winter large-pan evaporation contributed in proportions of 40%, 32%, 20%, and 8%, respectively. This sharp rebound in large-pan evaporation was mainly caused by recent spring and summer heat wave and drought events, which increased concurrent air temperature, VPD, and sunshine hours. Our finding of rapid rebound in pan evaporation alerts us to promptly adopt appropriate mitigating strategies of water and crop managements to cope with increasing extreme climate events.

Acknowledgments

This research was supported by the Strategic Priority Research Program of the Chinese Academy of Sciences (XDA19040303), the

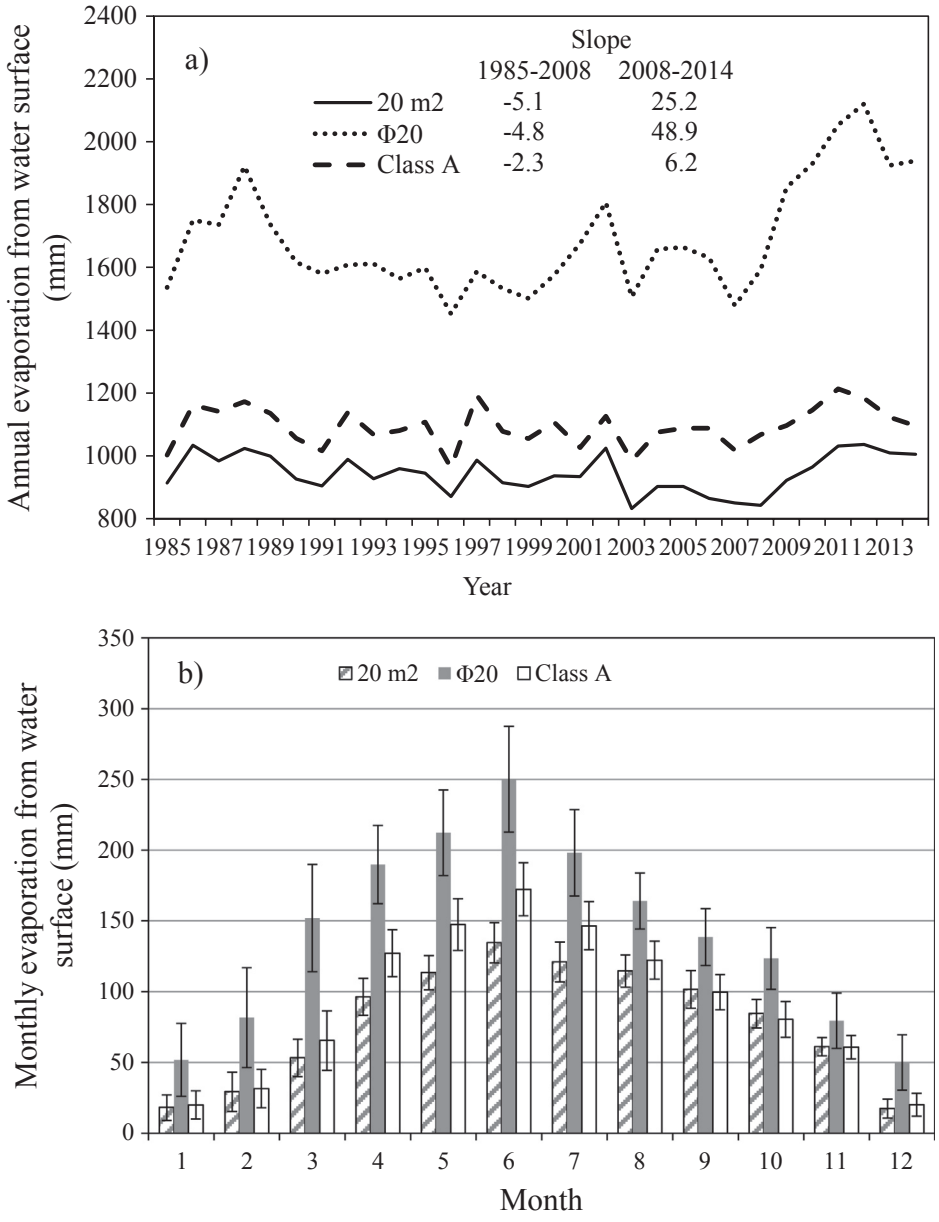

Fig. 10. Yearly a) and monthly b) pan evaporation records of the large pan, the Φ20 evaporation pan, and the Class A pan at the YCES station.

National Key Research and Development Program of China (2017YFC0503805), National Natural Science Foundation of China (31570472), and the 100 Talents Program of the Chinese Academy of Sciences. Authors appreciate Mr. Zhenmin Liu and Mr. Yanchun Yu for their contributions on data collection and preprocessing.

Appendix A. Supplementary data

Supplementary data associated with this article can be found, in the online version, at https://doi.org/10.1016/j.jhydrol.2018.08.014.

References

Abtew, W., Obeysekera, J., Iricanin, N., 2011. Pan evaporation and potential evapotranspiration trends in South Florida. Hydrol. Processes 25 (6), 958–969.
Brena-Naranjo, J.A., Laverde-Barajas, M.A., Pedrozo-Acuna, A., 2017. Changes in pan evaporation in Mexico from 1961 to 2010. Int. J. Climatol. 37 (1), 204–213.
Brutsaert, W., Parlange, M.B., 1998. Hydrologic cycle explains the evaporation paradox. Nature 396 (6706) 30 30.
Burn, D.H., Hesch, N.M., 2007. Trends in evaporation for the Canadian prairies. J. Hydrol. 336 (1–2), 61–73.
Chin, D.A., Zhao, S.F., 1995. Evaluation of Evaporation-Pan Networks. J. Irrig. Drain. Eng. -ASCE 121 (5), 338–346.
Douglas, E.M., et al., 2006. Changes in moisture and energy fluxes due to agricultural land use and irrigation in the Indian Monsoon Belt. Geophys. Res. Lett. 33 (14), L14403.
Eriksson, L., et al., 2006. Multi- and Megavariate Data Analysis-Part I Basic Principles and Applications, 3rd ed. MKS Umetrics AB.
Fu, G.B., Liu, C.M., Chen, S.L., Hong, E.L., 2004. Investigating the conversion coefficients for free water surface evaporation of different evaporation pans. Hydrol. Processes 18 (12), 2247–2262.
Golubev, V.S., et al., 2001. Evaporation changes over the contiguous United States and the former USSR: a reassessment. Geophys. Res. Lett. 28 (13), 2665–2668.
IPCC, 2013. Climate change 2013: The Physical Science Basis. Contribution of Working Group I to the Fifth Assessment Report of the Intergovernmental Panel on. Climate Change.
Jhajharia, D., Shrivastava, S.K., Sarkar, D., Sarkar, S., 2009. Temporal characteristics of pan evaporation trends under the humid conditions of northeast India. Agric. For. Meteorol. 149 (5), 763–770.
Kisi, O., 2015. An innovative method for trend analysis of monthly pan evaporations. J. Hydrol. 527, 1123–1129.
Li, Z., Chen, Y., Shen, Y., Liu, Y., Zhang, S., 2013. Analysis of changing pan evaporation in the arid region of Northwest China. Water Resour. Res. 49 (4), 2205–2212.
Lim, W.H., Roderick, M.L., Farquhar, G.D., 2016. A mathematical model of pan evaporation under steady state conditions. J. Hydrol. 540, 641–658.
Limjirakan, S., Limsakul, A., 2012. Trends in Thailand pan evaporation from 1970 to

2007. Atmos. Res. 108, 122–127.
Liu, M., Shen, Y., Zeng, Y., Liu, C., 2010. Trend in pan evaporation and its attribution over the past 50 years in China. J. Geog. Sci. 20 (4), 557–568.
Liu, X., Luo, Y., Zhang, D., Zhang, M., Liu, C., 2011a. Recent changes in pan-evaporation dynamics in China. Geophys. Res. Lett. 38 (13), L13404.
Liu, X., Zheng, H., Zhang, M., Liu, C., 2011b. Identification of dominant climate factor for pan evaporation trend in the Tibetan Plateau. J. Geog. Sci. 21 (4), 594–608.
McVicar, T.R., et al., 2012. Global review and synthesis of trends in observed terrestrial near-surface wind speeds: implications for evaporation. J. Hydrol. 416, 182–205.
Ohmura, A., Wild, M., 2002. Is the hydrological cycle accelerating? Science 298 (5597), 1345–1346.
Ogolo, E.O., 2011. Regional trend analysis of pan evaporation in Nigeria (1970 to 2000). J. Geogr. Reg. Plann. 4 (10), 566–577.
Pereira, A.R., Nova, N.A.V., Pereira, A.S., Barbieri, V., 1995. A model for the class-a pan coefficient. Agric. For. Meteorol. 76 (2), 75–82.
Peterson, T.C., Golubev, V.S., Groisman, P.Y., 1995. Evaporation losing its strength. Nature 377 (6551), 687–688.
Roderick, M.L., Farquhar, G.D., 2002. The cause of decreased pan evaporation over the past 50 years. Science 298 (5597), 1410–1411.
Roderick, M.L., Farquhar, G.D., 2004. Changes in Australian pan evaporation from 1970 to 2002. Int. J. Climatol. 24 (9), 1077–1090.
Roderick, M.L., Rotstayn, L.D., Farquhar, G.D., Hobbins, M.T., 2007. On the attribution of changing pan evaporation. Geophys. Res. Lett. 34 (17), L17403.
Rotstayn, L.D., Roderick, M.L., Farquhar, G.D., 2006. A simple pan-evaporation model for analysis of climate simulations: evaluation over Australia. Geophys. Res. Lett. 33 (17), L17715.
Sherwood, S., Fu, Q., 2014. A drier future? Science 343 (6172), 737–739.
Tao, F.L., Zhang, Z., Zhang, S., Rotter, R.P., 2016. Variability in crop yields associated with climate anomalies in China over the past three decades. Reg. Environ. Change 16 (6), 1715–1723.
Vicente-Serrano, S.M., Bidegain, M., Tomas-Burguera, M., Dominguez-Castro, F., El Kenawy, A., McVicar, T.R., Azorin-Molina, C., Lopez-Moreno, J.I., Nieto, R., Gimeno, L., Gimenez, A., 2018. A comparison of temporal variability of observed and model-based pan evaporation over Uruguay (1973–2014). Int. J. Climatol. 38 (1), 337–350.
Wang, K.C., Dickinson, R.E., Liang, S.L., 2012. Global Atmospheric Evaporative Demand over and from 1973 to 2008. J. Clim. 25 (23), 8353–8361.
Wang, T., Zhang, J., Sun, F., Liu, W., 2017. Pan evaporation paradox and evaporative demand from the past to the future over China: a review. Wiley Interdiscip. Rev.: Water 4 (3), E1207.
Wang, Y.W., Yang, Y.H., 2014. China's dimming and brightening: evidence, causes and hydrological implications. Ann. Geophys. 32 (1), 41–55.
Wild, M., 2009. Global dimming and brightening: a review. J. Geophys. Res. 114, D11D16.
Xie, H., Zhu, X., Yuan, D., 2015. Pan evaporation modelling and changing attribution analysis on the Tibetan Plateau (1970–2012). Hydrol. Processes 29 (9), 2164–2177.
Yang, H., Yang, D., 2012. Climatic factors influencing changing pan evaporation across China from 1961 to 2001. J. Hydrol. 414–415, 184–193.
Yesilirmak, E., 2013. Temporal changes of warm-season pan evaporation in a semi-arid basin in Western Turkey. Stochastic Environ. Res. Risk Assess. 27 (2), 311–321.
You, G.Y., Zhang, Y.P., Liu, Y.H., Song, Q.H., Lu, Z.Y., Tan, Z.H., Wu, C.S., Xie, Y.N., 2013. On the attribution of changing pan evaporation in a nature reserve in SW China. Hydrol. Processes 27 (18), 2676–2682.
Yu, H.Y., Xu, J.C., Okuto, E., Luedeling, E., 2012. Seasonal response of grasslands to climate change on the tibetan plateau. PLoS One 7 (11), E49230.
Yuan, Z., Yan, D.H., Yang, Z.Y., Yin, J., Yuan, Y., 2015. Temporal and spatial variability of drought in Huang-Huai-Hai River Basin, China. Theor. Appl. Climatol. 122 (3–4), 755–769.
Zhang, Q., Qi, T., Li, J., Singh, V.P., Wang, Z., 2015. Spatiotemporal variations of pan evaporation in China during 1960–2005: changing patterns and causes. Int. J. Climatol. 35 (6), 903–912.
Zhang, Y., Liu, C., Tang, Y., Yang, Y., 2007. Trends in pan evaporation and reference and actual evapotranspiration across the Tibetan Plateau. J. Geophys. Res. 112 (D12), D12110.